Food & Function

Protein-polyphenol interactions enhance the antioxidant capacity of phenolics: Analysis of rice glutelin-procyanidin dimer interactions

Journal:	*Food & Function*
Manuscript ID	FO-ART-11-2018-002246.R1
Article Type:	Paper
Date Submitted by the Author:	29-Dec-2018
Complete List of Authors:	Dai, Taotao; Nanchang University, State Key Laboratory of Food Science and Technology Chen, Jun; Nanchang University, State Key Laboratory of Food Science and Technology McClements, David; University of Massachusetts, Food Science Hu, Peng; Nanchang University, State Key Laboratory of Food Science and Technology Ye, Xiaoqin; Nanchang University, State Key Laboratory of Food Science and Technology Liu, Chengmei; Nanchang University, State Key Laboratory of Food Science and Technology Li, Ti; Nanchang University, State Key Laboratory of Food Science and Technology

Protein-polyphenol interactions enhance the antioxidant capacity of phenolics: Analysis of rice glutelin-procyanidin dimer interactions

Taotao Dai[a], Jun Chen[a], David Julian McClements[b]*, Peng Hu[a], Xiaoqin Ye[a], Chengmei Liu[a], Ti Li[a]*

[a] *State Key Laboratory of Food Science and Technology, Nanchang University, No. 235 Nanjing East Road, Nanchang 330047, China*

[b]*Department of Food Science, University of Massachusetts, Amherst, MA 01003, USA*

Corresponding author:

*Ti Li

E-mail address: liti@ncu.edu.cn

Tel: 86-13330060958

Fax: +86-791- 8334509

*David Julian McClements

E-mail address: mcclements@foodsci.umass.edu

Tel: (413) 545-1019

Fax: (413) 545-1262

ABSTRACT

Rice glutelin and procyanidins are often used in functional foods as sources of plant-based proteins and polyphenols, respectively, but little is currently known about the interactions between them. In our research, the interaction between rice glutelin and B-type procyanidin dimer (PB2) were investigated. The presence of the PB2 decreased the α-helix and random coil structure of the rice protein and reduced its surface hydrophobicity. However, PB2 did not adversely affect the functional performance of RG in the emulsions. Conversely, the antioxidant capacity of the PB2 was enhanced in the presence of the rice protein. Fluorescence spectroscopy confirmed that the protein and PB2 formed molecular complexes, which were primarily the result of hydrophobic attractive forces. Molecular docking analysis provide insights into the nature of the interaction between the rice protein and PB2. This study provides valuable insights into the nature of the interactions between plant proteins and polyphenolic nutraceuticals.

Keywords: rice glutelin, procyanidins dimer, spectroscopy, conformation, antioxidant capacity, molecular docking

Introduction

Proanthocyanidins are the most common subtype of flavonoids [1]. They are a class of oligomers and polymers consisting of flavan-3-ol monomer units held together by A-type or B-type linkages, which are commonly found in fruits, vegetables, legumes, wine, nuts, rice [2, 3]. Because of their excellent antioxidant capacities and other potential health benefits, proanthocyanidins have attracted considerable attention from researchers [4-6]. However, the application of proanthocyanidins in foods is limited because of their physicochemical instability [7, 8]. Environmental conditions are known to impact the chemical stability of proanthocyanidins, including ambient oxygen levels, temperature, light exposure, and system composition [8, 9]. Previous studies have reported that the stability of proanthocyanidins can be enhanced by forming proanthocyanidin-protein complexes [7, 8, 10].

Numerous studies indicate that proanthocyanidins have high binding affinities for proteins, such as digestive enzymes, salivary proteins, bovine serum albumin, gelatin, and lysozyme [11, 12]. Recently, there has been considerable interest in increasing the utilization of plant proteins in foods because of potential benefits in terms of health, ethical, and sustainability issues [13, 14]. Consequently, it is important to understand how proanthocyanidins interact with plant proteins.

Rice proteins are regarded as a valuable source of plant proteins due to their relatively high digestibility and biological value, making them particularly suitable candidates to replace dairy and soy proteins in infant formula, nutritional beverages,

and other protein-rich products [15, 16]. However, little is currently known about the interactions between rice proteins and polyphenols. Wang et al. reported that the conformation and surface hydrophobicity of rice proteins were changed by addition of polyphenols (Thunb. leaf pigments), and that the antioxidant capacity of the protein decreased [17]. Meng et al. reported that the conformation of rice bran protein isolate changed after interaction with polyphenols (tea catechins), and that the protein improved the stability of the tea catechins [18]. But, the nature of the protein-polyphenol interactions was not characterized in these studies. Clearly, further research is required to elucidate the precise mechanisms involved in the formation of plant protein-polyphenol complexes.

Glutelin is the main protein fraction in rice, which is composed of two major polypeptide subunits, with molecular weights of 30-40 kDa (α or acidic) and 19-23 kDa (β or basic) [16]. Procyanidins are the most common proanthocyanidins founds in foods, which have also been reported to have potential health benefits such as antioxidant, anticancer, anti-inflammatory, and cardioprotective activities [2]. For this reason, rice glutelin (RG) was used as a model rice protein and a pure procyanidin compound (PB2, epicatechin unit and B-type linked dimer, Fig 1D) was selected as a model proanthocyanidin. The molecular interactions between these two plant-based components was studied using various spectroscopic methods, including fluorescence, circular dichroism (CD), and ultraviolet (UV), as well as computational docking simulation. Moreover, the impact of the protein-polyphenol interaction on the

antioxidant activity of the PB2 and the functional performance of RG in the emulsions were determined. The research is possible to gain some useful insight into the interaction mechanism of plant proteins and polyphenolic nutraceuticals in foods.

Materials and methods

Materials

Rice protein (purity>90%) was obtained from JiangXi Golden Agriculture Biotech Co., Ltd. B-type procyanidins dimer (CAS No: 29106-49-8) was purchased from Aladdin Industrial Company. (Shanghai, China). 1-anilinonaphthalene-8-sulfonic acid (ANS), fluorescein isothiocynate (FITC), 1,1-diphenyl-2-picrylhydrazyl free radical (DPPH), 2, 4, 6-tris (2-pyridyl)-s-triazine (TPTZ) were obtained from Sigma-Aldrich Chemical Inc. (St. Louis, MO, USA). Flaxseed oil was purchased from a local commercial food supplier. Bradford protein assay kit was purchased from Beyotime Biotechnology (Shanghai, China). All other chemical reagents were analytical grade and purchased from Aladdin Industrial Company. (Shanghai, China). Ultrapure water was utilized throughout the research.

Preparation of samples

Stock PB2 solutions were prepared in phosphate buffer (PB, 0.01 mol/L, pH 7.0) at room temperature. These solutions were then diluted with phosphoate buffer to obtain a range of PB2 concentrations (0.05 to 3.46 mmol/L). The rice glutelin

extraction method was based on one reported previously [19], with a few minor modifications. In brief, rice glutelin was extracted from rice protein by the sequential extraction of the albumin, globulin, prolamin, and glutelin fractions with ultrapure water, 50% NaCl, 70% ethanol, and 0.1 mol/L NaOH. The protein content of the rice glutelin obtained was 93.5% (dry basis), which was measured by the Kjeldahl method (*N*%×5.95). Rice glutelin powder was dissolved in phosphate buffer (0.01 mol/L, pH 7.0) to obtain a stock solution at a 4.20 mg/mL BSA equivalent, which was measured using a Bradford protein assay kit. Both PB2 and RG stock solutions were filtered before analysis through 0.45 μm filters (WondaDisc MCE, Shimadzu-gl).

PB2 antioxidant activities by chemical-based assays

Two different antioxidant models (DPPH and FRAP) were employed to evaluate the effect of protein-polyphenol complexation on the antioxidant activity of the PB2. Aliquots (0.2 mL) of solutions containing different PB2 levels were added to 3.0 mL of 0.84 mg/mL RG solution to prepare RG-PB2 mixed solutions. The final concentrations of PB2 in these mixtures were 6.75, 13.50, 27.01, 54.02, and 108.03 × 10^{-3} mol/L. All samples were placed in centrifuge tubes that were exposed to the natural environment for zero or two days.

DPPH radical scavenging assay

The DPPH radical scavenging capacity of RG-PB2 was measured according to the method described by Duan et al. [20], with some slight modifications. 0.3 mL of RG-PB2

mixed sample was added to 3.0 mL of 24 mg/L DPPH reagent. PB was used as a blank for the PB2 solution, while rice glutelin solution was used as a blank for the RG-PB2 mixed solution. The absorbance of the mixtures after 30 min in a dark environment was determined at 517 nm by UV spectrophotometer (TU-1901, Persee, Beijing, China). The DPPH radical scavenging capacity was assessed using the following formula:

$$\text{DPPH radical scavenging capacity (\%)} = (1-A_0/A_1)\times 100 \quad (1)$$

Here, A_1 is the absorbance of the control and A_0 is the absorbance of samples.

Ferric-reducing antioxidant power (FRAP) assay

The ferric-reducing antioxidant power of RG-PB2 was measured, according to the method described by Benzie and Strain [21], with some modifications. The principle of this method is based on the reduction of the ferric complex in 2, 4, 6-tripyridil-s-triazine (Fe^{3+}-TPTZ) to the ferrous form (Fe^{2+}-TPTZ). In brief, the FRAP reagent was prepared from sodium acetate buffer (0.3 mol/L, pH 3.6), 0.02 mol/L $FeCl_3$ solution and 0.01 mol/L TPTZ solution (0.04 mol/L HCl as solvent) in a volume ratio of 10:1:1, respectively. The FRAP reagent was freshly prepared daily and warmed to 37 ^oC prior to use. A 0.3 mL RG-PB2 solution was added to 3.0 mL FRAP reagent. Again, PB was used as a bank for the PB2 solution, while rice glutelin solution were used as blank for the RG-PB2 mixed solution. The absorbance of the samples was measured at 593 nm by a UV spectrophotometer, after 15 min incubation at 37 ^oC. The phenolic antioxidant capacity was expressed as Vc (mg/mL) using a calibration curve (0-150 mg/L).

Circular dichroism determination

Circular dichroism spectra were recorded using a CD spectrometer (MOS-450, Claix, France), according to the method described by Arroyo-Maya et al. [22]. A quartz cuvette with a 1.0 mm optical path length was used to contain the samples. Briefly, 0.2 mL PB2 solution (0-1.73×10^{-3} mol/L) were added to 3.0 mL RG solution (4.20 mg/mL). All spectra of RG-PB2 mixtures were scanned in the far-UV range between 190 and 250 nm at room temperature (25 ±1 ^{o}C). The spectra obtained using the appropriate PB2 blank was then subtracted to correct the background. The contents of the α-helix, β-sheet, β-turn, and random coil of RG were calculated using the CONTIN method in DICHROWEB (http://dichroweb.cryst.bbk.ac.uk/html/home.shtml).

UV spectra measurements

UV spectra of samples were scanned on a UV spectrophotometer, according to the method described by Cai et al. [23], with some slight modifications. Briefly, A 0.2 mL PB2 solution (0-1.73×10^{-3} mol/L) was added to 3.0 mL RG solution (0.84 mg/mL). The absorption spectrum was collected from 190 to 400 nm and then the spectrum from the corresponding PB2 blank was subtracted to correct the background.

Fluorescence quenching assay

The fluorescence emission spectra of samples were measured using a fluorescence spectrofluorimeter (F-7000, Hitachi, Tokyo, Japan) equipped with a thermostat bath and 1.0 cm optical path length quartz cuvette. The influence of PB2 on RG in the

formation of protein-phenolic complexes was quantified by the intrinsic fluorescence quenching method described previously by Dai et al. [24]. In brief, the fluorescence emission spectra of RG-PB2 mixture samples were recorded at 298, 304, and 310 K, respectively, using an excitation wavelength of 280 nm and excitation and emission slit widths of 2.5 nm. Synchronous fluorescence spectrometry was used to characterize changes in the local environment of the tyrosine and tryptophan residues in the RG. Fluorescence scanning was carried out using a setting of $\Delta\lambda$=15 nm and $\Delta\lambda$=60 nm for tyrosine and tryptophan, respectively. A 0.2 mL aliquot of PB2 solution (0-1.73×10^{-3} mol/L) was added to 3.0 mL of RG solution (0.84 mg/mL). All the mixtures were agitated then equilibrated for 30 min before carrying out the measurements. The fluorescence intensity of the samples was determined and then the appropriate PB2 blank was subtracted to correct for background fluorescence. In addition, the fluorescence spectra of RG with PB2 was measured to demonstrate the formation of a RG-PB2 non-fluorescence complex. Furthermore, the intrinsic fluorescence data were utilized to investigate the fluorescent quenching mechanism between RG and PB2.

Surface hydrophobicity measurements

Changes in surface hydrophobicity of RG-PB2 mixtures were measured using ANS as a fluorescence probe and a F-7000 spectrofluorimeter to collect the signals according to the method described by Cao et al. [25], with some slight modifications, using an excitation wavelength of 390 nm and excitation and emission slit widths of 5.0

and 2.5 nm, respectively. Then, 16 μL of 8 mmol/L ANS solution was added to 3.2 mL of RG-PB2 mixtures. These latter solutions were formed by mixing 3.0 mL of RG solution (4.20 mg/mL) with 0.2 mL of PB2 solutions with a range of concentrations. In addition, the PB2 solution was used as blank. The surface hydrophobicity of rice glutelin was expressed as the relative ANS-fluorescence intensity [26].

Particle size measurements

The particle size distributions of rice glutelin and RG-PB2 solution (3.0 mL RG with 0.2 mL 1.73 mmol/L PB2) were determined using a Zetasizer Nano ZSP (Malvern Instrument, Ltd., U.K.). All measurements were carried out at 25 °C and 37°C.

Computational docking simulation

Computational docking simulations were performed according to the method described by Dai et al. [27], with some slight modifications, utilizing the LibDock algorithm of the Discovery Studio 3.0 program (BIOVIA, United States). The 3D structures of PB2 were then displayed using ChemBio3D Ultra 17.0. The homology modeling method was used to construct the 3D structure of RG [28]. The sequence alignment between rice glutelin (GI: 20221) and pumpkin seed globulin (PDB: 2EVX) revealed the highest sequence identity of 46% [24, 29]. In general, the homology model structure of the rice glutein can be utilized in molecular docking studies, if the sequence identity of the rice glutein and pumpkin seed globulin is near 40% [30]. Some preprocessing was done on the structure of rice glutein, including removed water

molecules and added all hydrogen atoms according the "Prepare Protein" module at pH 7.0. To obtain a lowest energy minimized conformation, the PB2 molecule was optimized use the *small molecule module* at pH 7.0. The CHARMm force field algorithm was added to the molecular structure of PB2 and RG. The RG and PB2 were set as receptor and ligand, respectively. The number of hotspots was set at 100 and the docking tolerance was 0.25. The interaction between PB2 and RG were observed. The result of docking resulted in 10 poses, and the best pose was selected which based on the reported LibDock scores.

Emulsion preparation

A coarse oil-in-water emulsion was prepared by homogenizing 10 wt% flaxseed oil with 90 wt% aqueous rice glutelin solution (2 wt%, pH 7.0) and rice glutelin with procyanidin (2 wt% rice glutelin, 0.02% procyanidin) using a high-shear mixer at 10,000 rpm for 2 min (M133/1281-0, Biospec Products, Inc., ESGC, Switzerland), followed by passing through a microfluidizer (M110P, Microfluidics, Newton, MA) at 12,000 psi for 3 passes. Finally, 0.02% (w/w) of sodium azide was added as a microbial preservative.

Particle size measurements

The particle size distribution of the emulsions was analyzed by laser light scattering (Mastersizer 2000; Malvern Instruments, Worcestershire, UK). To avoid multiple scattering, samples were diluted with a buffer solution with the same pH and

ionic composition as the sample being measured. Particle size data is presented as the surface-weighted mean diameter (d_{32}) calculated from the particle size distribution.

ζ-potential measurements

The ζ-potential of the particles in the samples was determined by particle electrophoresis (Zetasizer Nano ZS-90, Malvern Instruments, Worcestershire, UK). To avoid multiple scattering effects, emulsions were diluted 250-fold using buffer solutions with the same pH and ionic composition as the samples.

Confocal laser scanning microscopy (CLSM)

Confocal fluorescent microscopy images of the emulsions were acquired using an optical microscope (Leica TCS SP5, Leica Microsystems, Wetzlar, Germany) using a HCX PLAPO 60 × oil immersion objective at room temperature. 1 mL of emulsion was stained with 50 μL Nile Red solution (1 mg/mL in ethanol) and 50 μL FITC (10 mg/mL in dimethyl sulfoxide) to dye the oil and protein, respectively. A drop of sample was placed on a slide for visualization. Fluorescent dyes were excited using an argon 488 nm laser and the emitted light was measured at 515 nm for protein and 621 nm for oil, respectively.

Statistical analysis

A comparison of the means was performed by Tukey's test using one-way analysis of variance. The statistical analyses were carried on SPSS version 25.0 (SPSS Inc., Chicago, IL).

Results and discussion

Fluorescence emission spectrum

Measurements of the fluorescence spectra of RG in the presence of various PB2 levels were used to provide information about protein-polyphenol interactions at different temperatures (Fig. 1). A strong fluorescence emission peak was observed for RG around 345 nm. The fluorescence intensity from the RG decreased appreciably when the PB2 level was increased, whereas there was only a slight shift in the wavelength where the maximum peak occurred (ca. 2 nm). These results indicated that PB2 quenches the intrinsic fluorescence of the RG.

When the PB2 level reached 0.58×10^{-3} mol/L, the RG-PB2 solution had little fluorescence (Fig. 1D). This phenomenon may be the result of the formation of non-fluorescent RG-PB2 complexes where the microenvironment of the tyrosine and tryptophan residues in the RG are altered. Previous researchers have reported that the fluorescence intensity of various other proteins (including β-lactoglobulin and bovine serum albumin) also decreased when increasing amounts of phenolics were added (such as pelargonidin and erucic acid), which was again attributed to the interaction between the protein and polyphenols [22, 31].

The mean diameter of the particles in the RG and RG-PB2 solutions did not change significantly (Table 1), with most of them being around 90 nm at both 25 and 37 °C. The particle size data therefore suggests that the RG-PB2 complexes were relatively

stable. Taken together, the results of the fluorescence and particle size measurements indicated that PB2 and RG formed stable non-fluorescent complexes.

Analysis of fluorescence quenching of RG with PB2

Fluorescence quenching due to molecular interactions can be categorized as either static or dynamic [32]. Fluorescence quenching data of RG with PB2 was analyzed using the Stern-Volmer equation (1), which is useful for elucidating the origin of the fluorescence quenching mechanism [33]:

$$\frac{F_0}{F} = 1 + K_q \tau_0 [Q] = 1 + K_{SV} [Q] \qquad (1)$$

Here, F_0 and F denote the fluorescence intensities of RG before and after addition of PB2, respectively; [Q] is the quencher (PB2) concentration; K_{SV} represents the Stern-Volmer quenching constant; K_q is the biomolecular quenching rate constant and τ_0 (10^{-8} s) is the average lifetime of the fluorophore in the absence of a quencher [32].

The Stern-Volmer plot in Fig. 1E indicated good linearity (R^2>0.99) at the three temperatures used, suggesting that quenching was either due to a collisional or a static mechanism [34]. The K_{SV} (K_{SV}=$K_q\tau_0$) values [1.46×10^4 (298 K), 1.80×10^4 (304 K), and 2.23×10^4 L·mol^{-1} (310 K)] increased gradually as the temperature rose (Table 2), suggesting the main interaction between PB2 and RG was hydrophobic [34].

From Fig. 1E, the smallest K_q (1.46×10^{12} L·mol^{-1}·s^{-1}) is significantly higher than the maximum diffusion collision quenching constant (2.0×10^{10} L·mol^{-1}·s^{-1}), suggesting the static quenching was occurring [35]. For static quenching, a double logarithmic

equation (2) can be used to calculate the binding constant (K_a) of the interaction between quenchers (PB2) and protein (RG), and the number (n) of binding sites per protein [36].

$$\log \frac{F_0 - F}{F} = \log K_a + n \log[Q] \quad (2)$$

As shown in Table 2, the n values plotted by eq. (2) were all approximately equal to 1 indicating that RG had a single class of binding site for PB2. Others results attained from the analysis of Fig. 1F are summarized in Table 2. The binding constant (K_a) was calculated using eq. (2). The K_a values [0.55×10^5 (298 K), 1.52×10^5 (304 K), and 2.47×10^5 L·mol^{-1} (310 K)] of the RG-PB2 complexes increased upon increasing temperature. In comparison with the K_a (0.36×10^4, 0.81×10^4, and 1.13×10^4 L·mol^{-1} under 298 K, 304 K, and 310 K, respectively) between gallic acid and rice glutelin [24], PB2 had a stronger affinity to rice glutelin than gallic acid.

Hydrogen bonds, hydrophobic interactions, and electrostatic forces are believed to play an important role in protein-ligand formation. The enthalpy change (ΔH), entropy change (ΔS), and free energy change (ΔG) were calculated to provide some insights into the main forces contributing to the protein-polyphenol interactions in our study. Previous studies suggest that hydrogen bonds are involved in the interaction when $\Delta H < 0$ and $\Delta S < 0$; hydrophobic forces dominate when $\Delta H > 0$ and $\Delta S > 0$; and electrostatic forces dominate when $\Delta H < 0$ and $\Delta S > 0$ [37]. The ΔH, ΔS and ΔG values were calculated using the Van't Hoff equation [35].

$$\ln K_a = -\frac{\Delta H}{RT} + \frac{\Delta S}{R} \quad (3)$$

$$\Delta G = \Delta H - T\Delta S \quad (4)$$

Where T is the absolute temperature (298, 304, and 310 K), K_a is the binding constant obtained from eq. 2, and R is the gas constant (8.314 J·mol^{-1}·K^{-1}). The ΔH and ΔS values were obtained from the slope and intercept of the linear plots of lnK_a versus 1/T. ΔG was then calculated from equation (4).

The negative ΔG values shown in Table 2 suggest that the binding of RG with PB2 was spontaneous. The values of ΔH and ΔS for the binding interaction were +96.0 kJ·mol^{-1} and +0.39 kJ·mol·K^{-1}, respectively. This suggests that hydrophobic forces were therefore the main type of interaction between RG and PB2. This result is in accord with earlier studies that indicated the driving forces for the binding of flavonoids (such as procyanidin and pelargonidin) to proteins (such as mucin and β-lactoglobulin) involved mainly hydrophobic interactions [22, 33].

Effect of complex formation on surface hydrophobicity of RG

An ANS fluorescent probe was used to measure the binding sites and monitor the exposed non-polar surface groups on the protein. Surface hydrophobicity was detected by relative ANS-binding fluorescence intensities of RG in the absence and presence of PB2. The surface hydrophobicity of RG decreased gradually with increasing PB2 concentration (Fig. 2). This decrease in surface hydrophobicity was linked to the reduction in exposed hydrophobic groups on the rice glutelin surface.

Presumably, the presence of PB2 prevents ANS binding to RG hydrophobic surface. This result is consistent with that of Xu et al. [29], who reported a decrease in surface hydrophobicity of glutelin due to interactions with hydrophobic zones on amylose. The data from the ANS binding studies is also in agreement with the data obtained from the thermodynamic analysis described earlier.

Effect of complex formation on RG conformation

Conformational changes of RG were characterized by the simultaneous scanning of excitation and emission monochromators using a fluorometer [38]. At $\Delta\lambda$ values of 60 and 15 nm, the synchronous fluorescence spectra provide information about microenvironment changes for tryptophan and tyrosine residues, respectively. The synchronous fluorescence spectra of RG solutions in the presence of different concentrations PB2 are shown in Figs. 3A and 3B. The fluorescence intensity of tryptophan is markedly stronger than tyrosine, suggesting that tryptophan was the main contributor to RG fluorescence. The fluorescence intensity from the tryptophan and tyrosine decreased with increasing PB2 concentration. Moreover, when the PB2 concentration was 27.01×10^{-6} mol/L, the decrease in intensity was significantly larger ($p<0.05$) for tyrosine (41.42% ± 0.87%) than for tryptophan (24.30% ± 0.93%). This result indicates that tyrosine contributed more than tryptophan to the binding process, and that tyrosine was much closer to the binding sites than tyrosine. This inference is supported by the computational docking simulation results shown in Fig. 6C. At both

$\Delta\lambda$ values, there was a conspicuous red shift (ca. 9 nm) of the λ_{max} when PB2 was added to the RG. This red shift indicates that the polarity of the microenvironment of the phenolic amino acids residues was altered, which may have occurred due to a protein conformation change leading to exposure of more tryptophan and tyrosine residues to the surrounding water [39].

CD is a sensitive technique to monitor conformational changes of proteins. CD spectra of RG were therefore recorded in the absence and presence of PB2 (Fig. 3C). The negative ellipticity of the RG decreased when the PB2 concentration was increased, implying some secondary structural changes occurred in the protein. The secondary structure contents of RG were calculated from the spectra (Fig. 3C). In the absence of the polyphenol, the pure RG had around 10.8% α-helix, 33.4% β-sheet, 22.9% β-turn, and 33.0% random coil, which agrees with previous studies [29]. After interaction with 108×10^{-6} mol/L PB2, the amounts of α-helix decreased (to 6.4%), random coil decreased (to 30.6%) and β-sheet increased (to 39.7%). A decrease in the content of α-helix structure may be because PB2 inserted itself into the hydrophobic surfaces of the RG molecules and destroyed its hydrogen bonding networks [40]. The results correlated well with the analyses of surface hydrophobicity discussed in earlier sections.

UV spectroscopy analysis

The UV spectrum of proteins provides valuable information about structural changes and intermolecular interactions [41]. The UV spectra of RG solutions

containing different PB2 levels were therefore measured (Fig. 3D). The RG had an absorption peak around 275 nm, which can be attributed to the formation of a π-π transition peptide bond involving the C=O group in tyrosine and tryptophan. With an increase in PB2 concentration from 3.38 to 108×10^{-6} mol/L, the RG's absorption progressively increased. Our results agree with earlier studies that reported a change in α-amylase UV spectra in the presence of procyanidins due to binding interactions [23]. Presumably, the interaction of RG with PB2 changed the microenvironment of the tryptophan and tyrosine residues. Again, these results correlate well with the analyses of the conformational changes discussed in the earlier sections.

Influence on complex formation on the antioxidant activity of PB2

Two different antioxidant models (DPPH and FRAP) were employed to evaluate the influence on complex formation on the antioxidant activity of PB2. Both DPPH (Fig. 4A) and FRAP (Fig. 4B) showed that the antioxidant activity of the PB2 solution decreased after exposure to the environment for 2 days. This loss of antioxidant became less pronounced as the PB2 concentration increased. The presence of the protein greatly increased the stability of the PB2, which was seen in both the DPPH and FRAP models. These results demonstrate that the antioxidant activity of PB2 can be protected by complexation with RG. We postulate that when PB2 interacts with RG through hydrophobic forces, there is less opportunity for pro-oxidants in the environment to interact with the polyphenol molecules.

Influence on complex formation on the rice glutelin emulsion

The impact of forming complexes between the protein and polyphenol on the functional properties of the protein was established by measuring the particle size, ζ-potential, and confocal microscopy images of 10% flaxseed oil-in-water emulsions stabilized by either 2% protein or 2% protein + polyphenol during storage at ambient temperature for 14 days (Figs. 5). All the emulsions were physically stable throughout storage with no evidence of droplet aggregation seen in the light scattering or microscopy data, and no visible evidence of creaming. Overall, these results showed that the polyphenols did not adversely affect the functional performance of these protein in the emulsions.

Computational docking studies

A molecular docking simulation was used to identify and visualize the binding sites of PB2 in the RG. The method used (LibDock docking algorithm) is a high throughput approach that positions catalyst-generated PB2 conformations in the RG active site, based on the presence of hotspots, *i.e.,* polar interaction sites [42]. The highest Libdock score we obtained for the protein-polyphenol interactions was 80.90 (Table 3). The most stable conformation pose was selected for molecular docking analysis. The 3D molecular docking mode (Fig. 6A and B) and 2D interaction diagram (Fig. 6C) indicate that PB2 inserted itself into a cavity on the RG surface and interacted with some amino acid residues. Fig. 6C suggests that PB2 was mainly surrounded by 14

amino acid residues on the rice protein, including Tyr 429, Met 417, Ala 411, Leu 439, Leu 410, Ile 386, Val 358, Val 385, Val 359, Val 384, Gln 357, Met 334, Arg 388, Pro 337. Five hydrophobic interaction forces (Pi-Alkyl) were found between aromatics rings of PB2 and alkyl groups of amino acid residues (Pro 337, 6.05 Å, Leu 410, 5.38 Å, Ile 386, 4.85 Å, Val 359, 3.91 Å, Val 384, 4.42 Å). One hydrogen bond was also found between the hydroxyl groups of PB2 and the H-acceptor sites of Val 359, 3.93 Å. The dominant interaction force was found to be hydrophobic in origin, which agreeds with the results of the thermodynamic analysis. Furthemore, the PB2 located near the active site as shown in Fig. 6A, and the active amino acids included Arg 447, Val 335, Lys 387, His 338, Ser 345. The PB2 also interacted with the amino acid Tyr 429, leading to a change in conformation of the RG, which was again consistent with the results of our analyitical measurements of the protein conformational changes.

Ackonwledgements

The authors thank the National Nature Science Foundation of China (31460394, 31760441), the Jiangxi Province Postgraduate Innovation Fund (YC2017-B012). This material was partly based upon work supported by the National Institute of Food and Agriculture, USDA, Massachusetts Agricultural Experiment Station (MAS00491)

References

1. P. Ravindranathan, D. Pasham, U. Balaji, J. Cardenas, J. Gu, S. Toden and A. Goel, Mechanistic insights into anticancer properties of oligomeric proanthocyanidins from grape seeds in colorectal cancer, *Carcinogenesis*, 2018, **39**, 767-777.
2. E. A. Rue, M. D. Rush and R. B. van Breemen, Procyanidins: a comprehensive review encompassing structure elucidation via mass spectrometry, *Phytochem. Rev.*, 2018, **17**, 1-16.
3. J. Serrano, R. Puupponen-Pimia, A. Dauer, A. M. Aura and F. Saura-Calixto, Tannins: Current knowledge of food sources, intake, bioavailability and biological effects, *Mol. Nutr. Food Res.*, 2009, **53**, S310-S329.
4. P. Ravindranathan, D. Pasham, U. Balaji, J. Cardenas, J. Gu, S. Toden and A. Goel, A combination of curcumin and oligomeric proanthocyanidins offer superior anti-tumorigenic properties in colorectal cancer, *Sci. Rep.*, 2018, **8**, 13869.
5. X. H. Yang, T. Liu, B. Chen, F. Q. Wang, Q. F. Yang and X. H. Chen, Grape seed proanthocyanidins prevent irradiation-induced differentiation of human lung fibroblasts by ameliorating mitochondrial dysfunction, *Sci. Rep.*, 2017, **7**, 62.
6. C. Blade, G. Aragones, A. Arola-Arnal, B. Muguerza, F. I. Bravo, M. J. Salvado, L. Arola and M. Suarez, Proanthocyanidins in health and disease, *Biofactors*, 2016, **42**, 5-12.
7. C. Z. Liu, M. Li, J. Yang, L. Xiong and Q. J. Sun, Fabrication and characterization of biocompatible hybrid nanoparticles from spontaneous co-assembly of casein/gliadin and proanthocyanidin, *Food Hydrocolloid*, 2017, **73**, 74-89.

8. Z. K. Zhou, G. Y. Sun, Y. Q. Lui, Y. J. Gao, J. J. Xu, D. M. Meng, P. Strappe, C. Blanchard and R. Yang, A novel approach to prepare protein-proanthocyanidins nano-complexes by the reversible assembly of ferritin cage, *Food Sci. Technol. Res.*, 2017, **23**, 329-337.

9. Z. Xu, L. H. Wei, Z. Z. Ge, W. Zhu and C. M. Li, Comparison of the degradation kinetics of A-type and B-type proanthocyanidins dimers as a function of pH and temperature, *Eur. Food Res. Technol.*, 2015, **240**, 707-717.

10. M. H. Grace, I. Guzman, D. E. Roopchand, K. Moskal, D. M. Cheng, N. Pogrebnyak, I. Raskin, A. Howell and M. A. Lila, Stable binding of alternative protein-enriched food matrices with concentrated cranberry bioflavonoids for functional food applications, *J. Agric. Food Chem.*, 2013, **61**, 6856-6864.

11. N. P. Ulrih, Analytical techniques for the study of polyphenol-protein interactions, *Crit. Rev. Food Sci. Nutr.*, 2017, **57**, 2144-2161.

12. L. Jakobek, Interactions of polyphenols with carbohydrates, lipids and proteins, *Food Chem.*, 2015, **175**, 556-567.

13. T. Chalvon-Demersay, D. Azzout-Marniche, J. Arfsten, L. Egli, C. Gaudichon, L. G. Karagounis and D. Tome, A systematic review of the effects of plant compared with animal protein sources on features of metabolic syndrome, *J. Nutr.*, 2017, **147**, 281-292.

14. L. Day, Proteins from land plants-Potential resources for human nutrition and food security, *Trends Food Sci. Technol.*, 2013, **32**, 25-42.

15. Q. Zhao, H. Xiong, C. Selomulya, X. D. Chen, H. L. Zhong, S. Q. Wang, W. J. Sun and Q. Zhou, Enzymatic hydrolysis of rice dreg protein: Effects of enzyme type on the

functional properties and antioxidant activities of recovered proteins, *Food Chem.*, 2012, **134**, 1360-1367.

16. L. Amagliani, J. O'Regan, A. L. Kelly and J. A. O'Mahony, The composition, extraction, functionality and applications of rice proteins: A review, *Trends Food Sci. Technol.*, 2017, **64**, 1-12.
17. L. Wang, Y. Xu, S. M. Zhou, H. F. Qian, H. Zhang, X. G. Qi and M. H. Fan, Interaction between *Vaccinium bracteatum* Thunb. leaf pigment and rice proteins, *Food Chem.*, 2016, **194**, 272-278.
18. M. Shi, L. Y. Huang, N. Nie, J. H. Ye, X. Q. Zheng, J. L. Lu and Y. R. Liang, Binding of tea catechins to rice bran protein isolate: Interaction and protective effect during in vitro digestion, *Food Res. Int.*, 2017, **93**, 1-7.
19. L. Lei, Q. Zhao, C. Selomulya and H. Xiong, The effect of deamidation on the structural, functional, and rheological properties of glutelin prepared from *Akebia trifoliata* var. *australis* seed, *Food Chem.*, 2015, **178**, 96-105.
20. X. Duan, M. Li, H. J. Ma, X. M. Xu, Z. Y. Jin and X. B. Liu, Physicochemical properties and antioxidant potential of phosvitin-resveratrol complexes in emulsion system, *Food Chem.*, 2016, **206**, 102-109.
21. I. F. F. Benzie and J. J. Strain, The ferric reducing ability of plasma (FRAP) as a measure of "antioxidant power": The FRAP assay, *Anal. Biochem.*, 1996, **239**, 70-76.
22. I. J. Arroyo-Maya, J. Campos-Teran, A. Hernandez-Arana and D. J. McClements, Characterization of flavonoid-protein interactions using fluorescence spectroscopy:

Binding of pelargonidin to dairy proteins, *Food Chem.*, 2016, **213**, 431-439.

23. X. Cai, J. N. Yu, L. M. Xu, R. Liu and J. Yang, The mechanism study in the interactions of sorghum procyanidins trimer with porcine pancreatic alpha-amylase, *Food Chem.*, 2015, **174**, 291-298.
24. T. T. Dai, X. Y. Yan, Q. Li, T. Li, C. M. Liu, D. J. McClements and J. Chen, Characterization of binding interaction between rice glutelin and gallic acid: Multi-spectroscopic analyses and computational docking simulation, *Food Res. Int.*, 2017, **102**, 274-281.
25. Y. Y. Cao and Y. L. Xiong, Interaction of whey proteins with phenolic derivatives under neutral and acidic ph conditions, *J. Food Sci.*, 2017, **82**, 409-419.
26. Y. Q. Li, Z. X. Chen and H. Z. Mo, Effects of pulsed electric fields on physicochemical properties of soybean protein isolates, *LWT-Food Sci. Technol.*, 2007, **40**, 1167-1175.
27. T. T. Dai, J. Chen, Q. Li, P. Y. Li, P. Hu, C. M. Liu and T. Li, Investigation the interaction between procyanidin dimer and alpha-amylase: Spectroscopic analyses and molecular docking simulation, *Int. J. Biol. Macromol.*, 2018, **113**, 427-433.
28. I. Lindin, Y. Wuxiuer, I. Kufareva, R. Abagyan, U. Moens, I. Sylte and A. W. Ravna, Homology modeling and ligand docking of Mitogen-activated protein kinase-activated protein kinase 5 (MK5), *Theor. Biol. Med. Model.*, 2013, **10**, 56.
29. X. F. Xu, W. Liu, J. Z. Zhong, L. P. Luo, C. M. Liu, S. J. Luo and L. Chen, Binding interaction between rice glutelin and amylose: Hydrophobic interaction and conformational changes, *Int. J. Biol. Macromol.*, 2015, **81**, 942-950.

30. D. Baker and A. Sali, Protein structure prediction and structural genomics, *Science*, 2001, **294**, 93-96.

31. Y. Shu, W. W. Xue, X. Y. Xu, Z. M. Jia, X. J. Yao, S. W. Liu and L. H. Liu, Interaction of erucic acid with bovine serum albumin using a multi-spectroscopic method and molecular docking technique, *Food Chem.*, 2015, **173**, 31-37.

32. J. R. Lakowicz and G. Weber, Quenching of protein fluorescence by oxygen. Detection of structural fluctuations in proteins on the nanosecond time scale, *Biochemistry*, 1973, **12**, 4171-4179.

33. E. Brandao, M. S. Silva, I. Garcia-Estevez, N. Mateus, V. de Freitas and S. Soares, Molecular study of mucin-procyanidin interaction by fluorescence quenching and Saturation Transfer Difference (STD)-NMR, *Food Chem.*, 2017, **228**, 427-434.

34. I. J. Joye, G. Davidov-Pardo, R. D. Ludescher and D. J. McClements, Fluorescence quenching study of resveratrol binding to zein and gliadin: Towards a more rational approach to resveratrol encapsulation using water-insoluble proteins, *Food Chem.*, 2015, **185**, 261-267.

35. L. Zeng, G. W. Zhang, S. Y. Lin and D. M. Gong, Inhibitory mechanism of apigenin on alpha-glucosidase and synergy analysis of flavonoids, *J. Agric. Food Chem.*, 2016, **64**, 6939-6949.

36. J. J. Jia, X. Gao, M. H. Hao and L. Tang, Comparison of binding interaction between beta-lactoglobulin and three common polyphenols using multi-spectroscopy and modeling methods, *Food Chem.*, 2017, **228**, 143-151.

37. P. D. Ross and S. Subramanian, Thermodynamics of protein association reactions - forces contributing to stability, *Biochemistry*, 1981, **20**, 3096-3102.

38. X. R. Li, G. K. Wang, D. J. Chen and Y. Lu, beta-Carotene and astaxanthin with human and bovine serum albumins, *Food Chem.*, 2015, **179**, 213-221.

39. H. X. Cheng, H. Liu, W. Bao and G. L. Zou, Studies on the interaction between docetaxel and human hemoglobin by spectroscopic analysis and molecular docking, *J. Photochem. Photobiol. B-Biol.*, 2011, **105**, 126-132.

40. Y. J. Wang, G. W. Zhang, J. H. Pan and D. M. Gong, Novel insights into the inhibitory mechanism of kaempferol on xanthine oxidase, *J. Agric. Food Chem.*, 2015, **63**, 526-534.

41. D. Zhong, Y. P. Jiao, Y. Zhang, W. Zhang, N. Li, Q. H. Zuo, Q. Wang, W. Xue and Z. H. Liu, Effects of the gene carrier polyethyleneimines on structure and function of blood components, *Biomaterials*, 2013, **34**, 294-305.

42. S. Singh, M. Awasthi, V. P. Pandey and U. N. Dwivedi, Lipoxygenase directed anti-inflammatory and anti- cancerous secondary metabolites: ADMET-based screening, molecular docking and dynamics simulation, *J. Biomol. Struct. Dyn.*, 2017, **35**, 657-668.

Figure captions:

Figure. 1 Fluorescence emission profiles of RG at various concentrations of PB2 at 298 K (**A**), 304 K (**B**), and 310K (**C**). **(D)** Fluorescence emission of RG at 0.58×10^{-3} mol/L PB2. **(E)** The Stern-Volmer plots for the quenching of RG by PB2 and the K_q of RG-PB2 complex in 298, 304 and 310 K, respectively. **(F)** The plots for the static quenching of RG by PB2 (298, 304, and 310 K). C_{RG}=0.84 mg/mL; C_{PB2}=0 to 0.11×10^{-3} mol/L).

Figure. 2 Changes in ANS-fluorescence intensity of RG at different concentrations of PB2. C_{RG}=4.20 mg/mL; C_{PB2}=0 to 0.22×10^{-3} mol/L.

Figure. 3 The synchronous fluorescence spectrum of RG in the absence and presence of PB2 at $\Delta\lambda$= 15 nm **(A)** and $\Delta\lambda$= 60 nm **(B)**, C_{RG}=0.84 mg/mL, C_{PB2}= 0 to 27.01×10^{-6} mol/L. T=298 K; **(C)** The contents of RG（4.8 mg/mL）secondary structure treated by PB2 with various PB2 concentrations (0.00, 27.01, 54.02, 108.03×10^{-6} mol/L); **(D)** Ultraviolet spectra of RG (0.84 mg/mL) treated by PB2 with various PB2 concentrations (from 0 to 216.06×10^{-6} mol/L).

Figure. 4 DPPH radical scavenging activity **(A)** and ferric-reducing antioxidant power **(B)** of PB2 and PB2+RG which were exposed in natural environment zero and two days.

Figure. 5 (A) Droplet diameter, (B) ζ-potential and (**C**) both photographs and confocal microscopy images of RG or RG-PB2 emulsions during storage time (14 days at room temperature).

Figure. 6 (A) 3D docking mode between PB2 and RG simulated by Discovery Studio and the amino acid of active site (Arg 447, Val 335, Lys 387, His 338, Ser 345); **(B)** the hydrophobic surface of protein receptor interact with PB2, the red colour and blue colour represent hydrophobicity and hydrophily, respectively; **(C)** 2D schematic interaction diagram between PB2 and RG, the colour of amino acid residue is drawn by interaction.

Table 1. Effect of PB2 on mean particle diameter (D) and polydispersity index (PDI) of rice glutelin at 25°C and 37 °C.

Protein Solution		25 °C	37 °C
RG	D (nm)	92.87±0.61[a]	93.13±1.78[a]
	PDI	0.29±0.01	0.28±0.01
RG-PB2	D (nm)	92.15±1.27[a]	94.13±1.37[a]
	PDI	0.30±0.02	0.28±0.01

The values of D were non-significantly different ($p > 0.05$).

Table 2. Quenching constants K_{SV}, binding constants K_a, and relative thermodynamic parameters for the interaction of PB2 with RG at different temperatures.

T(K)	K_{SV} ($\times 10^4$ L·mol^{-1})	K_a ($\times 10^4$ L·mol^{-1})	n	ΔG (kJ·mol^{-1})	ΔH (kJ·mol^{-1})	ΔS (kJ·mol^{-1}·K^{-1})	R^a
298	1.46±0.04[c]	0.553±0.001[c]	0.90±0.03	-21.55±0.36			
304	1.80±0.04[b]	1.522±0.001[b]	0.98±0.04	-23.92±0.01	95.99±18.43	0.39±0.06	0.9918
310	2.23±0.04[a]	2.469±0.001[a]	1.01±0.02	-26.29±0.37			

[a]R is the correlation coefficient for thermodynamic parameters. The values of K_{SV} and K_a were significantly different ($p < 0.05$) from each other in the same column.

Table 3. Parameters of LibDock protocol docking results

Pose number	1	2	3	4	5	6	7	8	9	10
LibDock Score	80.90	80.68	69.59	59.66	84.59	84.39	84.24	65.86	65.65	63.58

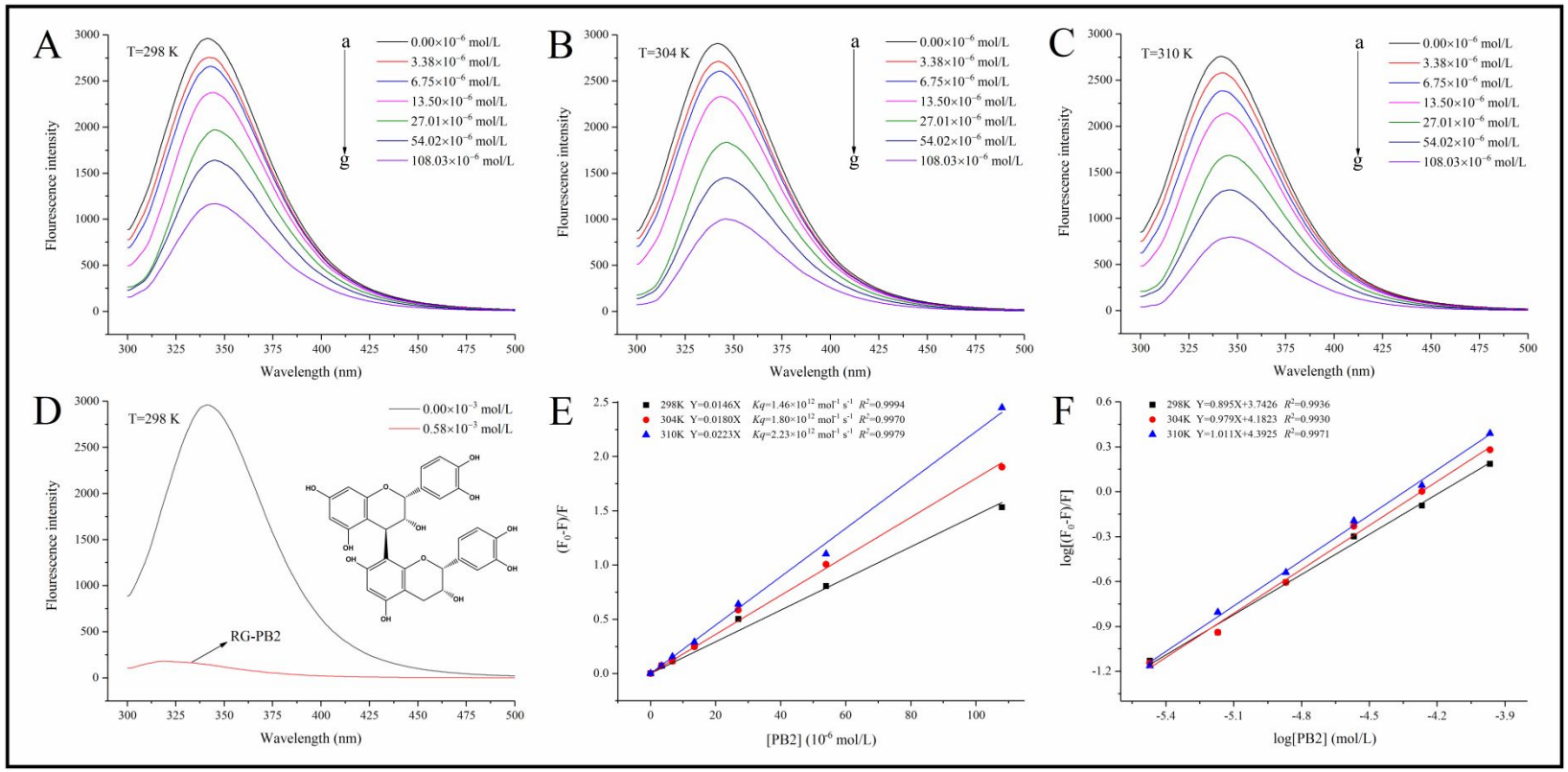

Figure. 1 Fluorescence emission profiles of RG at various concentrations of PB2 at 298 K (A), 304 K (B), and 310K (C). (D) Fluorescence emission of RG at 0.58×10^{-3} mol/L PB2. (E) The Stern-Volmer plots for the quenching of RG by PB2 and the Kq of RG-PB2 complex in 298, 304 and 310 K, respectively. (F) The plots for the static quenching of RG by PB2 (298, 304, and 310 K). C_{RG}=0.84 mg/mL; C_{PB2}=0 to 0.11×10-3 mol/L).

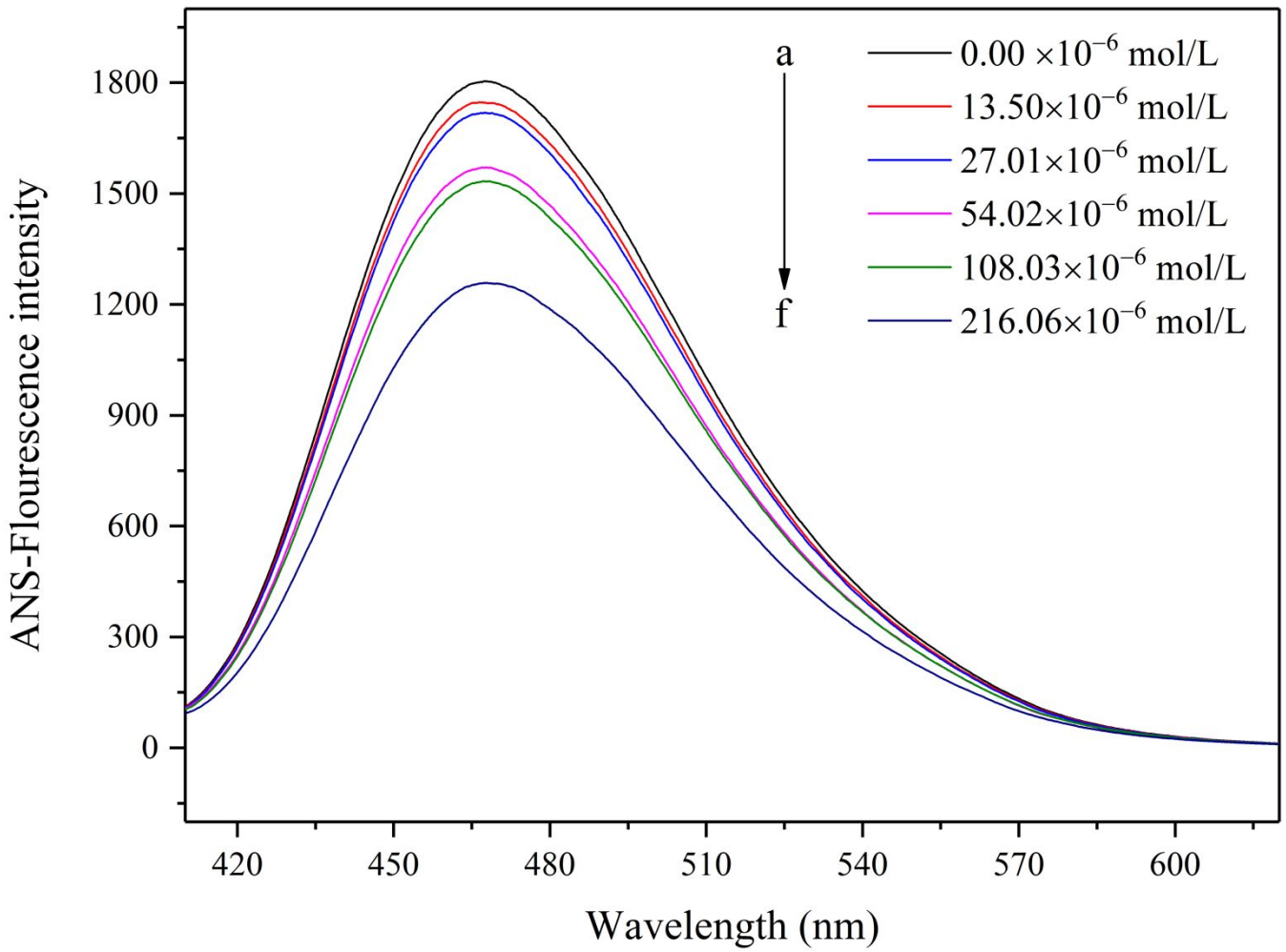

Figure. 2 Changes in ANS-fluorescence intensity of RG at different concentrations of PB2. C_{RG}=4.20 mg/mL; C_{PB2}=0 to 0.22×10^{-3} mol/L.

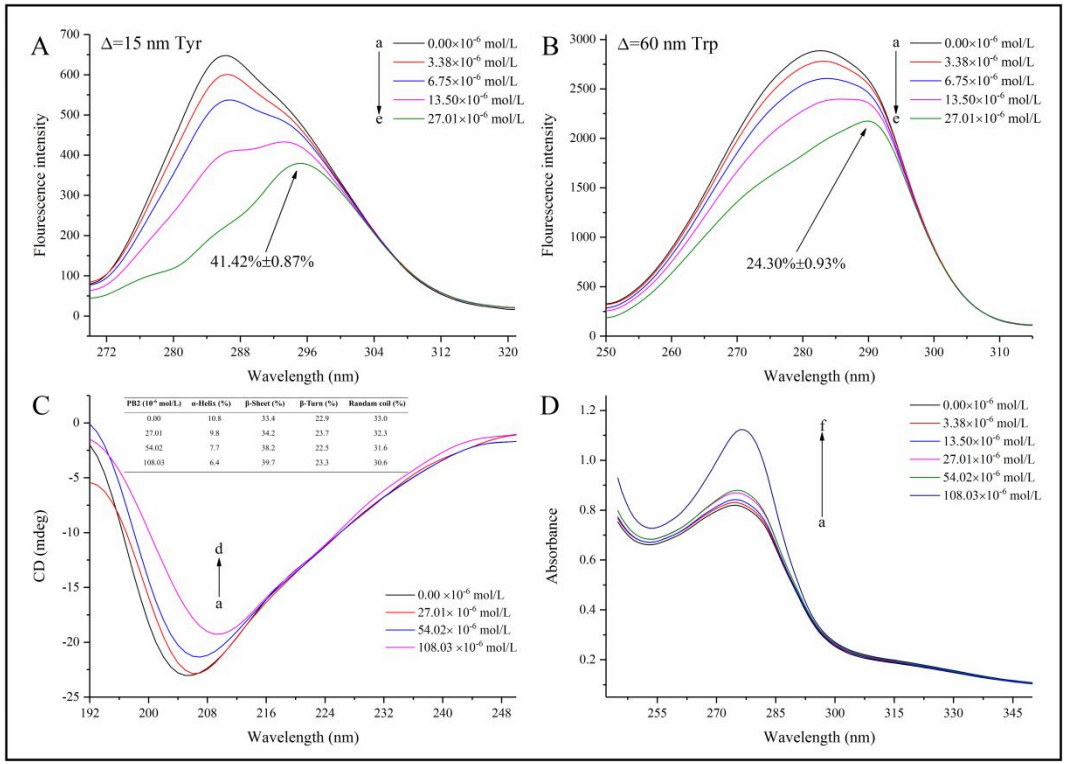

Figure. 3 The synchronous fluorescence spectrum of RG in the absence and presence of PB2 at Δλ= 15 nm **(A)** and Δλ= 60 nm **(B)**, C_{RG}=0.84 mg/mL, C_{PB2}= 0 to 27.01×10^{-6} mol/L. T=298 K; **(C)** The contents of RG（4.8 mg/mL）secondary structure treated by PB2 with various PB2 concentrations (0.00, 27.01, 54.02, 108.03×10^{-6} mol/L); **(D)** Ultraviolet spectra of RG (0.84 mg/mL) treated by PB2 with various PB2 concentrations (from 0 to 216.06 ×10^{-6} mol/L).

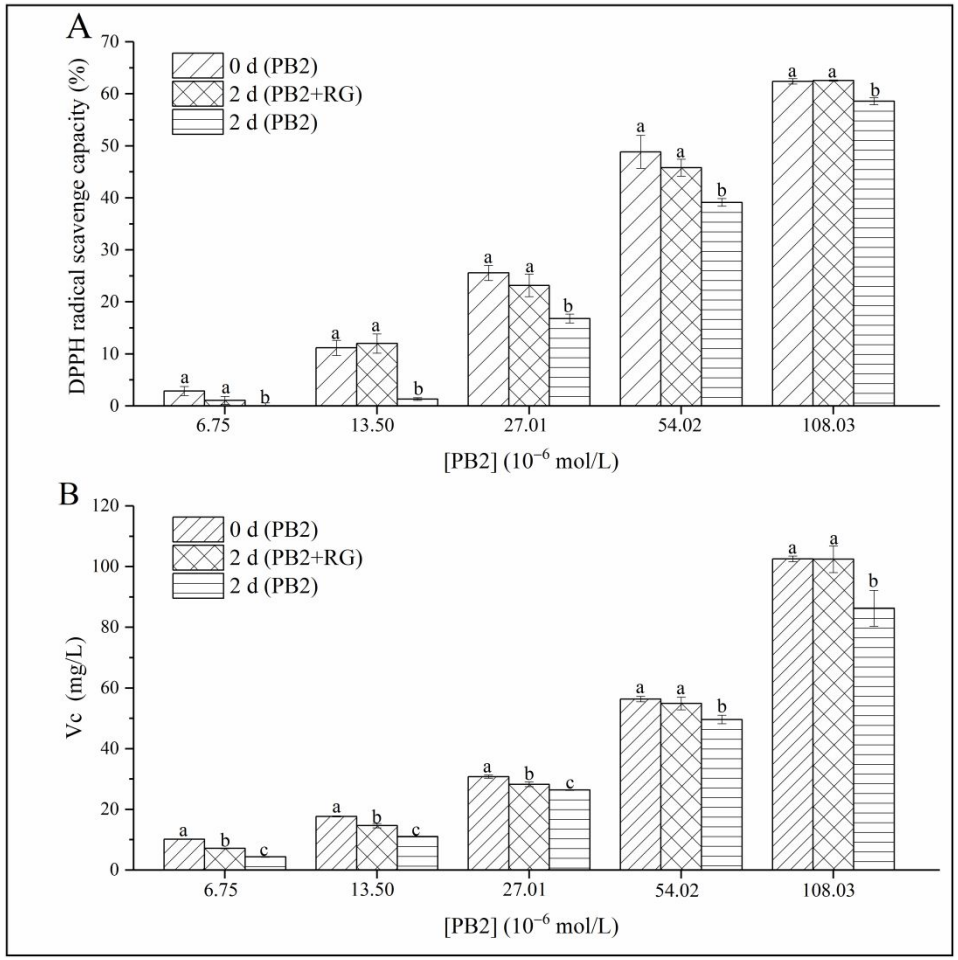

Figure. 4 DPPH radical scavenging activity **(A)** and ferric-reducing antioxidant power **(B)** of PB2 and PB2+RG which were exposed in natural environment zero and two days.

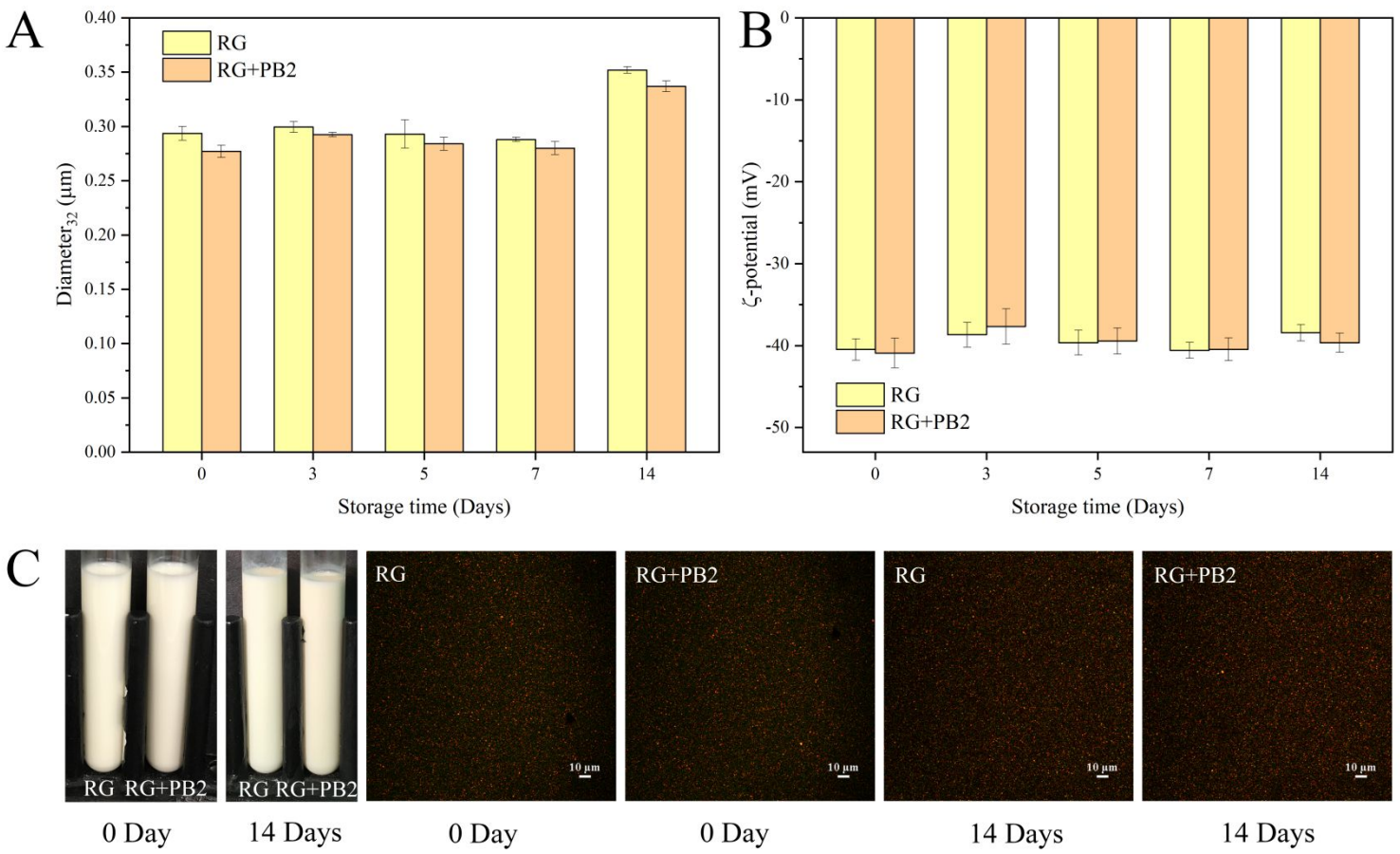

Figure. 5 (A) Droplet diameter, (B) ξ-potential and (C) both photographs and confocal microscopy images of RG or RG-PB2 emulsions during storage time (14 days at room temperature).

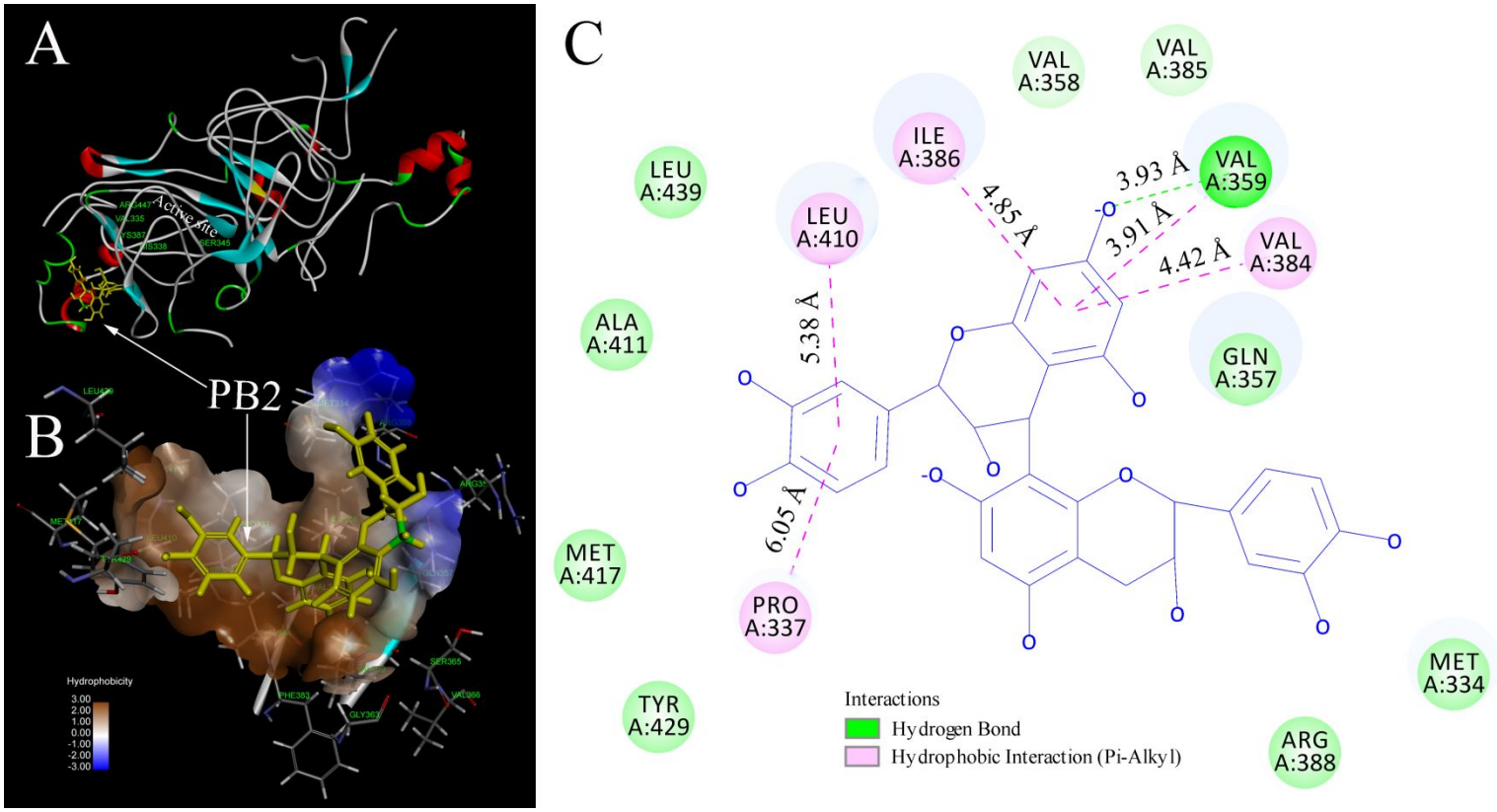

Figure. 6 (A) 3D docking mode between PB2 and RG simulated by Discovery Studio and the amino acid of active site (Arg 447, Val 335, Lys 387, His 338, Ser 345); **(B)** the hydrophobic surface of protein receptor interact with PB2, the red colour and blue colour represent hydrophobicity and hydrophily, respectively; **(C)** 2D schematic interaction diagram between PB2 and RG, the colour of amino acid residue is drawn by interaction.